Monitoring sealed automotive lead-acid batteries by sparse-impedance spectroscopy[¶]

B HARIPRAKASH, S K MARTHA and A K SHUKLA*
Solid State and Structural Chemistry Unit, Indian Institute of Science,
Bangalore 560 012, India
e-mail: shukla@sscu.iisc.ernet.in

Abstract. A reliable diagnostics of lead-acid batteries would become mandatory with the induction of an improved power net and the increase of electrically assisted features in future automobiles. Sparse-impedance spectroscopic technique described in this paper estimates the internal resistance of sealed automotive lead-acid batteries in the frequency range 10 Hz–10 kHz, usually produced by the alternators fitted in the automobiles. The state-of-health of the battery could be monitored from its internal resistance.

Keywords. Impedance spectroscopy; sealed lead-acid batteries; state-of-health; state-of-charge; internal resistance.

1. Introduction

The state-of-charge[α] (SOC) of a battery is reflected by the electrical response associated with the battery's resistance and inductance where the application of a load causes the battery voltage to drop instantaneously. This phenomenon has been targeted by researchers for determining the battery's resistance, and therefore, as an indicator of its discharged capacity. Since, open-circuit-voltage of a battery is a fixed quantity and its discharge circuit is also not altered, it is quite obvious that the internal resistance of the battery increases with its depth-of-discharge along with its voltage on-charge. Accordingly, if the discharge behaviour of the battery is known *a priori* then its state-of-health can be easily estimated. It is noteworthy that with the aging of the battery, the discharge capacity of the battery decreases owing to an increase in its internal resistance. Accordingly, the state-of-health[β] (SOH) of any sealed battery can be predicted from a knowledge of its internal resistance, which could be estimated from electrochemical impedance spectroscopy.

At present, the lead-acid battery is the most ubiquitous battery in the global rechargeable battery market and, in terms of value, the present world market for lead-acid batteries is about US$ 10 billion per annum.[1] The on-going electrification of automobiles makes a reliable diagnostic necessary for the vehicle's energy storage units. Since sealed
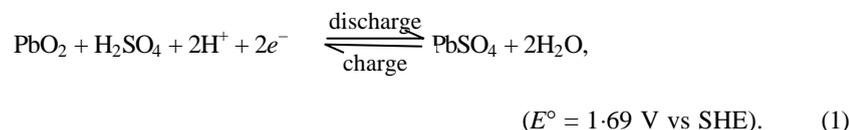
lead-acid batteries are supposed to become the most important battery storage technology for the near-term future vehicles, monitoring and diagnostic algorithm for these batteries are of great importance. Besides, with the induction of 36V/42V power net and the increase of electrically-assisted features e.g. idle/stop operation, launch assistance etc., the importance of a suitable battery monitoring and management will increase even further. In the literature, several methods are employed to monitor the SOH of various battery systems.[2–25] In this article, we describe on-line monitoring of sealed automotive lead-acid batteries by electrochemical sparse-impedance spectroscopy,[26] which is believed to find application in future automobiles.

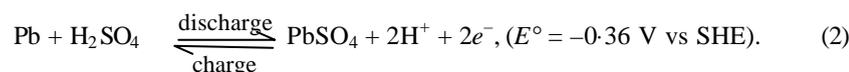## 2. Operating principle of sealed lead-acid batteries

The conventional flooded-type lead-acid battery requires checking of the specific gravity of the electrolyte, periodic addition of water to maintain electrolyte level above the plates and recharge soon after discharge to prevent hard sulphation that causes loss of capacity. The emission of acid fumes from these batteries causes corrosion of metallic parts in the vicinity of the battery. Furthermore, seepage of acid on the top cover of the batteries leads to leakage current resulting in increased self-discharge and ground-shunt hazard. To overcome these problems, valve-regulated lead-acid (VRLA) or sealed lead-acid (SLA) batteries based on a oxygen-recombination cycle have emerged. SLA batteries offer the freedom of battery placement, cyclability without the need for addition of water or checking the specific gravity, increased safety and superior performance in some instances.

The electrochemical reactions taking place at the positive and negative electrodes of a lead-acid battery are as follows.

At the positive electrode:

$$PbO_2 + H_2SO_4 + 2H^+ + 2e^- \underset{\text{charge}}{\overset{\text{discharge}}{\rightleftharpoons}} PbSO_4 + 2H_2O,$$

$$(E^\circ = 1\cdot69 \text{ V vs SHE}). \qquad (1)$$

At the negative electrode:

$$Pb + H_2SO_4 \underset{\text{charge}}{\overset{\text{discharge}}{\rightleftharpoons}} PbSO_4 + 2H^+ + 2e^-, (E^\circ = -0\cdot36 \text{ V vs SHE}). \qquad (2)$$

Accordingly, the net cell reaction is given by:

$$PbO_2 + Pb + 2H_2SO_4 \underset{\text{charge}}{\overset{\text{discharge}}{\rightleftharpoons}} 2PbSO_4 + 2H_2O, (E_{cell} = 2\cdot05 \text{ V}). \qquad (3)$$

Thermodynamic stability of the electrolyte requires that its lowest unoccupied state have a higher energy than the highest occupied state of the reductant and its highest occupied state have a lower energy than the lowest unoccupied state of the oxidant (figure 1).[27] If either of these two conditions is violated, electrons may be transferred to or from the electrolyte to reduce or oxidise it. Therefore, the requirement for thermodynamic stability of the electrolyte restricts the cell voltage (E_{cell}) to be always less than the thermodynamic window (E_g) of the electrolyte.
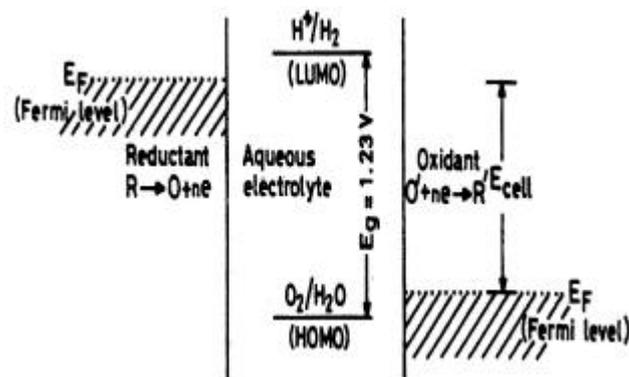
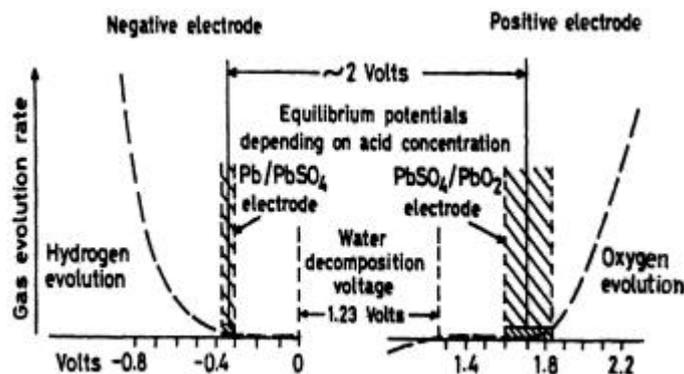**Figure 1.** Reaction window for an aqueous electrolyte electrochemical cell with solid metallic reactants.

Figure 2. Potential of $Pb/PbSO_4$ and $PbO_2/PbSO_4$ electrodes under equilibrium and during gas evolution.

Both PbO_2 and Pb are thermodynamically unstable in sulphuric acid solution. The equilibrium potential of $PbO_2/PbSO_4$ couple is more anodic to O_2/H_2O couple by 0·46 V and the equilibrium potential of $Pb/PbSO_4$ is more cathodic to H_2/H^+ couple by 0·36 V as shown in figure 2. Hence, even under open-circuit conditions, O_2 evolution at the PbO_2 electrode and H_2 evolution at the negative electrode can occur according to the reactions,

$$PbO_2 + H_2SO_4 \rightarrow PbSO_4 + H_2O + \tfrac{1}{2} O_2 \uparrow, \tag{4}$$

$$Pb + H_2SO_4 \rightarrow PbSO_4 + H_2 \uparrow. \tag{5}$$

The rates of reactions (4) and (5) increase with acid concentration. Therefore, the lead-acid cell should not work in principle but in practice however the high O_2 and H_2 overpotentials on PbO_2 and Pb enable the respective electrodes to be charged before O_2 and H_2 evolve at a substantial rate. In the lead-acid cell, it is the poor kinetics at the electrode–electrolyte interface that allows a cell voltage higher than the thermodynamic

window (E_g) of 1·23 V between the lowest unoccupied molecular orbital (LUMO) of the H_2/H^+ redox energy and the highest occupied molecular orbital (HOMO) of the O_2/H_2O redox energy.[28]

The positive electrode in a lead-acid cell accepts charge less efficiently than the negative electrode. Therefore, O_2 and H_2 are evolved non-stoichiometrically during the recharge of a lead-acid battery with O_2 evolution occurring prior to H_2 evolution. The oxygen evolved at the positive electrode is constantly reduced at the electrode as follows.

$$O_2 + 2Pb + 2H_2SO_4 \rightarrow 2PbSO_4 + 2H_2O. \tag{6}$$

This feature is the mainstay of the design of SLA batteries.[29]

3. Sparse-impedance spectroscopy on sealed lead-acid batteries

The electrical behaviour of battery half-cell can be described using the Randles equivalent circuit[4,26] shown in the figure 3a. In this case, only one electrode is modelled, but apart from different value for the parameters such as different time constants, the basic model can be used for both the electrodes. The equivalent circuit in figure 3a shows an ohmic resistance (R_i), which is due to the limited conductance of the contacts, the inter-cell connections, the electrodes and the electrolyte, and depends on the SOC of the battery, on its previous usage and on its age. The inductance (L) in figure 3a is mainly caused by the metallic connection (top lead) between poles and the electrodes of the battery, and the charge stored in the interface between the electrode and the electrolyte is modeled by the double-layer capacitance (C_{dl}). The kinetics of the main reaction by the non-linear charge-transfer resistance (R_{ct}), and finally diffusion is represented by the complex Warburg impedance (Z_w) in figure 3a.

In the frequency range between 1 kHz and 10 kHz, generally, only the inductance (L) and the internal resistance (R_i) are important because the other elements of the equivalent circuit have the double-layer capacitance in parallel, which is nearly ideally conducting in this frequency range. This leads to the strongly simplified equivalent circuit depicted in figure 3b. In this frequency range, the real part of the spectrum shows a noticeable
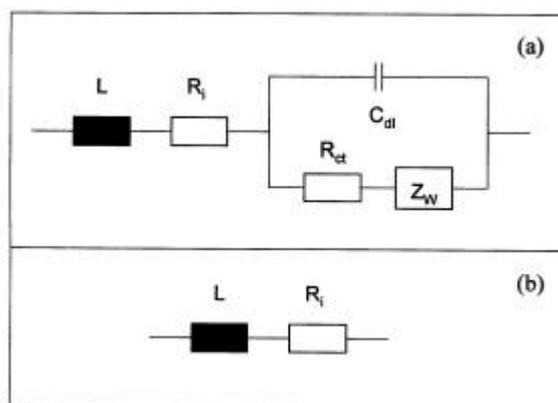

Figure 3. (a) Equivalent circuit for a battery half-cell and (b) high-frequency (≥ 1 kHz) equivalent circuit of a battery.
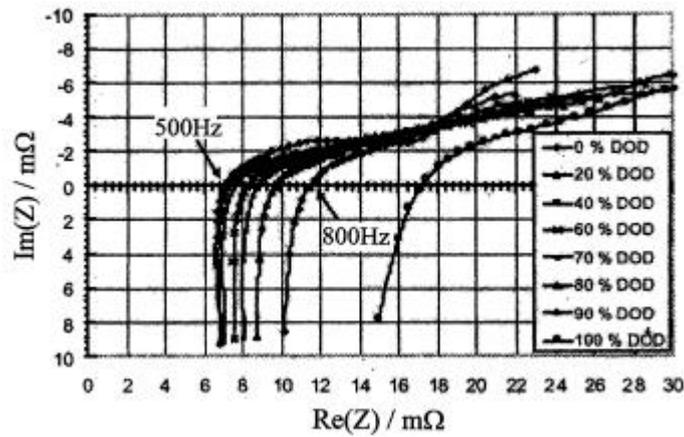
Figure 4. Impedance spectra of a 12 V/44Ah SLI battery at different depths-of-discharge (DOD) at 27°C with frequency ranging between 10 Hz and 6 kHz (after ref. [4]).
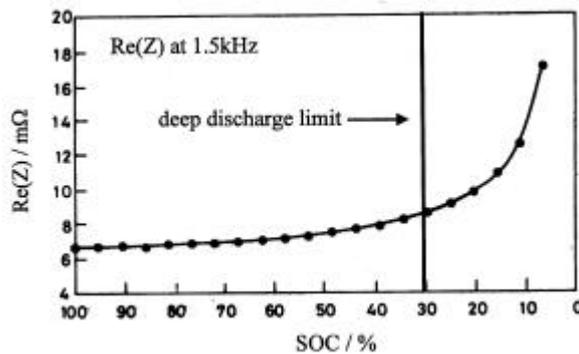

Figure 5. *Re*(Z) as function of state-of-charge at 1·5 kHz (after ref. [4]).

dependence on the SOC of the battery as shown in figure 4. The spectra are shifted to the right, i.e. the real part of the impedance, namely $Re(Z)$, becomes larger. Furthermore, the series resonance frequency, the frequency where the spectra cross the abscissa, increases from 500 to 800 Hz. For the determination of the ohmic internal resistance, the imaginary part of the spectrum, namely $I_m(Z)$, can be easily used. The $Re(Z)$ data in figure 4 can be expressed as a function of SOC as shown in figure 5. The SOC dependence of the internal resistance is not pronounced at high SOC level, whereas for a nearly discharged battery, the resistance increases rapidly. Although the internal resistance is mainly used as an indicator for the battery's cranking capability, the rapid increase in $Re(Z)$ can be used as an indicator to protect the battery against deep discharge during driving. Indeed, the data in figure 5 show that SOC below 30% is an easy indicator to estimate the SOH of the battery.

During impulse charging, e.g. cranking, the voltage drop at the non-linear resistive element R_{ct} with the capacitance in parallel follows with a remarkable time delay. Thus, the voltage response during short-time current peaks, e.g. cranking current, is dominated

by the ohmic resistance (R_i). Therefore, a method to determine the ohmic resistance (R_i) continuously during vehicular driving has been developed to measure small signal current and voltage excitations at the battery terminals. These small signal 'excitations' are already available in every vehicle's power supply system, and only passive measuring devices, e.g. current and voltage probes, are required.

An increase in the ohmic resistance of the battery is also observed with battery ageing. Poor SOH leads to an increased internal resistance (R_i). For a simple R_i measurement, SOC and SOH deviations, which might affect the internal resistance, cannot be distinguished but since the cranking capability is influenced by the sum of these, a separation is not actually necessary.

The following equations are employed in the basic algorithm for the determination of a battery's internal resistance.

$$R = \overline{P} / \overline{I}^2, \tag{7}$$

where

$$\overline{P} = \left(\int_{t}^{t+T} [u(t).i(t)] \mathrm{d}t \right) \div T, \tag{8}$$

and

$$\overline{I}^2 = \left(\int_{t}^{t+T} [i(t).i(t)] \mathrm{d}t \right) \div T. \tag{9}$$

In (7)–(9), R is the resistance, $\overline{P}$ is the time average value of the active power, $\overline{I}^2$ is the time average value of the square of the battery current, t refers to a particular time, T is the total time, $u(t)$ is the battery voltage at a particular time, and $i(t)$ is the battery current at a particular time.

The resistance is calculated by dividing the time average value of the active power by the time average of the square of the battery current. Before calculating (8) and (9), the current and voltage signals are band-pass filtered. The low-frequency components of the signals are removed in order to stay in the frequency range for which the simplified equivalent circuit can be used and very high frequencies have to be removed to stay within the limits of the sampling rate of the employed a/d converter. This measuring principle allows continuous and cost-effective determination of the battery's internal resistance over a wide frequency range.

The employed current sensor is designed to work in its measuring range during normal driving. The band-pass filtered voltage and current signals are both transmitted via a switched amplifier and a 'sample and hold' circuit to a/d converter of the microcontroller. After a/d conversion, the controller calculates the internal resistance according to (7)–(9), and obtains its average value over the measuring period. Furthermore, the controller provides a communication interface, which could send the latest value of the battery's internal resistance to the computing unit of the vehicle's battery management system responsible for interpretation of the measured resistance data. Figure 6 shows the minimum cranking voltage as function of the measured small signal internal resistance for the three series connected 12 V lead-acid batteries. The data in figure 6 suggest that by fixing the minimum cranking voltage, the battery can be protected against deep discharge, which ameliorates the battery's SOH.
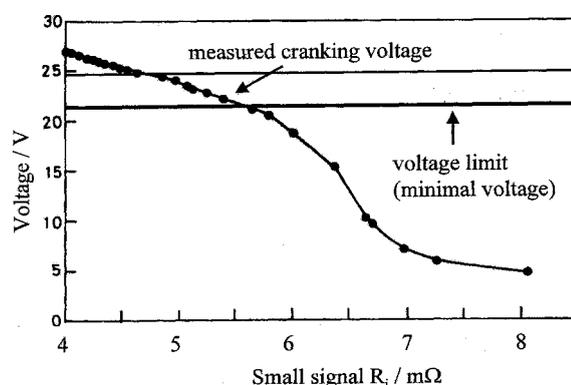
Figure 6. Minimum voltage during cranking as function of the measured small signal internal resistance at 27°C (after ref. [4]).

4. Conclusions

Electrochemical sparse-impedance spectroscopy has been found to be an appropriate technique for obtaining information about the SOH of sealed automotive lead-acid batteries. The technique facilitates the data collection on-board the vehicle, and the results are helpful in ameliorating the SOH of sealed automotive lead-acid batteries. It is believed that the sparse-impedance spectroscopic technique will find application in future automobiles to monitor the SOH of lead-acid battery bank.

References

1. Dell R M and Rand D A J 2002 *Understanding batteries* (Cambridge: Royal Society of Chemistry)
2. Fuet F 1998 *J. Power Sources* **70** 59
3. Piller S, Perrin M and Jossen A 2001 *J. Power Sources* **96** 113
4. Rodrigues S, Munichandraiah N and Shukla A K 2000 *J. Power Sources* **87** 12
5. Shukla A K, Ganesh Kumar V, Munichandraiah N and Srinath T 1998 *J. Power Sources* **74** 234
6. Champlin K and Bertness K 2000 *Proc. 22nd Int. Telecommun. Energy Conf.* (Phoenix: IEEE) paper 19.3 348
7. Charlesworth J M 1996 *Electrochim. Acta* **41** 1721
8. Nelatury S R and Singh P 2002 *J. Power Sources* **112** 621
9. Salkind A J, Fennie C, Singh P, Atwater T and Reisner D E 1999 *J. Power Sources* **80** 293
10. Stoynov Z, Nishev T, Vacheva V and Stamenova N 1997 *J. Power Sources* **64** 189
11. Martinet S, Durand R, Ozil P, Lablanc P and Blanchard P 1999 *J. Power Sources* **83** 93
12. Feder D O, Hlavac M J and McShane S J 1994 *J. Power Sources* **48** 135
13. Armenta C, Doria J, De Andrés M C, Urratia J, Fullea J and Graña F 1989 *J. Power Sources* **27** 189
14. Baert D H J and Vervaet A A K 2003 *J. Power Sources* **114** 357
15. Blood P J and Sotiropoulos S 2002 *J. Power Sources* **110** 96
16. Mancier V, Metrot A and Willmann P 2003 *J. Power Sources* **117** 223
17. Mancier V, Metrot A and Willmann P 2002 *Electrochim. Acta* **47** 1633
18. Hill I R and Andrukaitis Ed E 2001 *J. Power Sources* **103** 98
19. Mauracher P and Karden E 1997 *J. Power Sources* **67** 69
20. Jossen A, Späth V, Döring H and Garche J 1999 *J. Power Sources* **84** 283

21. Stoynov Z, Savova-Stoynov B and Kossev T 1990 *J. Power Sources* **30** 275
22. Salkind A, Atwater T, Singh P, Nelatury S, Damodar S, Fennie Jr C and Reisner D 2001 *J. Power Sources* **96** 151
23. Tenno A, Tenno R and Suntio T 2001 *J. Power Sources* **103** 42
24. Meissner E and Richter G 2003 *J. Power Sources* **116** 79
25. Karden E, Buller S, Rik W and De Doncker 2002 *Electrochim. Acta* **47** 2347
26. Buller S, Walter J, Karden E and De Doncker R W 2002 *Adv. Automotive Battery Conf.*, Las Vegas
27. Goodenough J B and Shukla A K 1988 *Solid state ionic devices* (eds) B V R Chowdhari and S Radhakrishna (Singapore: World Scientific) p. 573
28. Venugopalan S 1992 Ph D thesis, Indian Institute of Science, Bangalore
29. Linden D and Reddy T B (eds) 2002 *Handbook of batteries* 3rd edn (New York: McGraw-Hill)